Development 136, 1305-1315 (2009) doi:10.1242/dev.026922

Control of convergent yolk syncytial layer nuclear movement in zebrafish

Lara Carvalho[1], Jan Stühmer[1], Justin S. Bois[1,2], Yannis Kalaidzidis[1], Virginie Lecaudey[3] and Carl-Philipp Heisenberg[1,*]

Nuclear movements play an essential role in metazoan development. Although the intracellular transport mechanisms underlying nuclear movements have been studied in detail, relatively little is known about signals from surrounding cells and tissues controlling these movements. Here, we show that, in gastrulating zebrafish embryos, convergence movements of nuclei within the yolk syncytial layer (YSL) are guided by mesoderm and endoderm progenitors migrating along the surface of the yolk towards the dorsal side of the developing gastrula. Progenitor cells direct the convergence movements of internal yolk syncytial nuclei (iYSN) by modulating cortical flow within the YSL in which the iYSN are entrained. The effect of mesoderm and endoderm progenitors on the convergence movement of iYSN depends on the expression of E-cadherin, indicating that adhesive contact between the cells and the YSL is required for the mesendoderm-modulated YSL cortical flow mediating nuclear convergence. In summary, our data reveal a crucial function for cortical flow in the coordination of syncytial nuclear movements with surrounding cells and tissues during zebrafish gastrulation.

KEY WORDS: Gastrulation, Zebrafish, Nuclear movements, Yolk syncytial layer, Cortical flow

INTRODUCTION

Nuclear movements in eukaryotic cells are important for a wide variety of processes such as mitosis, meiosis, cell migration and cell polarization (Morris, 2000). Although in most cases nuclei are transported along microtubules by microtubule motor proteins (Morris, 2000; Morris, 2003; Reinsch and Gonczy, 1998), the actin cytoskeleton has also been implicated (Reinsch and Gonczy, 1998; Starr and Han, 2003). In addition to these intrinsic transport mechanisms, signals from surrounding tissues and cells have also been involved in nuclear movements. Notably, studies in *Drosophila* have provided evidence that the migration of the oocyte nucleus, which is required to establish the dorsal-ventral axis of the embryo, crucially depends on localized signals from the surrounding follicular epithelium (Gonzalez-Reyes et al., 1995; Roth et al., 1995).

Extensive nuclear movements have been observed within syncytial environments in metazoan development (D'Amico and Cooper, 2001; Englander and Rubin, 1987; Foe and Alberts, 1983; Trinkaus, 1993; Xiang and Fischer, 2004). One of the best-studied examples is the *Drosophila* syncytial preblastoderm, where nuclei initially move along the anterior-posterior axis of the embryo by actin-dependent cytoplasmic streaming and are subsequently transported towards the cortex along microtubules by associated motor proteins (Baker et al., 1993; Robinson et al., 1999; von Dassow and Schubiger, 1994). Although these studies have provided detailed insights into the molecular and cellular mechanisms that underlie syncytial nuclear migrations, much less is known about how such migrations are coordinated with the movements of surrounding cells and tissues in the developing organism.

[1]Max Planck Institute of Molecular Cell Biology and Genetics, Pfotenhauerstr. 108, 01307 Dresden, Germany. [2]Max-Planck-Institute for the Physics of Complex Systems, Nöthnitzer Str. 38, 01187 Dresden, Germany. [3]European Molecular Biology Laboratory, Cell Biology and Biophysics Department, Meyerhofstr. 1, 69126 Heidelberg, Germany.

*Author for correspondence (e-mail: heisenberg@mpi-cbg.de)

Accepted 11 February 2009

To obtain insights into the coordination of syncytial nuclear movements with surrounding cells and tissues, we have chosen to study the yolk syncytial layer (YSL) in the zebrafish gastrula. The YSL and its nuclei play crucial roles in embryo patterning and morphogenesis. Nodal/TGFβ signals emanating from the YSL are thought to be involved in specifying mesoderm and endoderm cell fates in marginal blastomeres along the circumference of the embryo (Chen and Kimelman, 2000; Mizuno et al., 1999; Mizuno et al., 1996; Ober and Schulte-Merker, 1999; Rodaway et al., 1999). Furthermore, interfering with the actin and microtubule cytoskeleton of the YSL leads to defective epiboly movements of both the YSL and the cellularized blastoderm (Cheng et al., 2004; Solnica-Krezel and Driever, 1994; Zalik et al., 1999), suggesting that proper YSL morphogenesis is required for blastoderm epiboly. Finally, the YSL has been proposed to induce fibronectin expression in the overlying embryonic tissue, which is important for heart progenitor cell migration during gastrulation and somitogenesis stages (Sakaguchi et al., 2006).

The YSL is formed by marginal blastomeres that collapse and deposit their nuclei into the cortical cytoplasm of the yolk cell at blastula stage (Kimmel and Law, 1985; Trinkaus, 1993). These yolk syncytial nuclei (YSN) undergo three to five rounds of divisions before ceasing mitosis at sphere stage. At this stage, the YSL contains several hundreds of YSN that can be subdivided into two main groups according to their position within the YSL (D'Amico and Cooper, 2001). External YSN (eYSN) form a marginal band of YSN located in front of the enveloping cell layer (EVL). Some of the eYSN move towards the vegetal pole (epiboly movements), whereas others recede from the marginal zone and undergo convergence and extension (CE) movements. By contrast, internal YSN (iYSN) are located below the blastoderm and EVL and primarily undergo CE movements. Strikingly, CE movements of iYSN appear very similar to the CE movements of the overlying blastoderm (mesoderm, endoderm and ectoderm progenitors) (D'Amico and Cooper, 2001). It has therefore been hypothesized that iYSN movements are driven by chemotactic signals emanating from overlying mesendoderm cells in the hypoblast (Cooper and Virta, 2007). Alternatively, iYSN may direct mesendoderm

movements, or iYSN and mesendoderm may move independently from each other (D'Amico and Cooper, 2001). However, direct experimental evidence for any of these hypotheses is still missing.

In this study, we show that the movements of mesendoderm progenitors and iYSN are coordinated during zebrafish gastrulation. Our findings suggest that mesendoderm progenitors direct iYSN movement by modulating cortical flow within the YSL responsible for nuclear transport. Furthermore, we show that the ability of mesendoderm progenitors to guide iYSN movements requires E-cadherin expression, suggesting that adhesive contact between mesendoderm progenitors and YSL is involved.

MATERIALS AND METHODS

Embryo staging and maintenance

Fish maintenance and embryo collection were carried out as described (Westerfield, 2000). Details can be provided on request.

Nuclear labeling

To label nuclei in live embryos, 1 mg/ml Histone H1 conjugated to Alexa Fluor 488 (H13188, Invitrogen) was injected in one marginal blastoderm cell at 16-cell stage (1.5 hours post-fertilization; hpf) to visualize mesendoderm progenitors, and in the YSL between high and sphere stage (3.3-4.0 hpf) to mark YSN.

mRNA injections

mRNA was synthesized and injected as described (Montero et al., 2005; Westerfield, 2000). Details can be provided on request.

Morpholino oligonucleotide injection

To knock down E-cadherin function, a previously described morpholino oligonucleotide designed against the 5′ end of e-cadherin cDNA (Babb and Marrs, 2004; Montero et al., 2005) (Gene Tools) was injected at the one-cell stage (0.25-0.5 ng).

Polystyrene microsphere injection

Fluoresbrite White-Green Microspheres (Polysciences Europe, Germany) with a diameter of 0.5 μm were washed twice in water by brief centrifugation and removal of the supernatant, then incubated for 1 hour in 0.1 μg/μl bovine serum albumin to block unspecific binding, briefly centrifuged and re-suspended in water. To insert microspheres into the YSL, a drop of 0.1 nl was injected at the margin of the YSL at 30% epiboly.

Transplantation experiments

MZoep mutant embryos were used as host embryos, and wild-type embryos were used as donor embryos. Between sphere and dome stage (4.0-4.3 hpf), dechorionated embryos were transferred into an agarose chamber. About 20 cells from a donor embryo were transferred into the blastoderm margin of a host *MZoep* embryo.

Cytochalasin and phalloidin treatment

For cytochalasin treatment, dechorionated 30-50% epiboly stage (5 hpf) embryos were incubated in 1-2 μg/ml cytochalasin B (Sigma-Aldrich, Germany) in 1× Danieau's buffer for 1-2 hours at 31°C. After treatment, embryos were mounted in low melting point (LMP) agarose containing cytochalasin. For phalloidin experiments, we injected into the YSL 100 pg *Lifeact-GFP m*RNA at the 1000-cell stage (3 hpf), 500 pg Histone-Alexa 488 at sphere stage (4 hpf) and 20 pg Amino-Phalloidin, Hydrochloride (Cat. No. ALX-350-266-M001, Alexis Biochemicals) at 50% epiboly.

Embryo sectioning and immunostaining

Embryos were sectioned and immunostained as described (Montero et al., 2005). Details can be provided on request.

Transmission electron microscopy

For analysis of the YSL ultrastructure, transmission electron microscopy was performed as described (Montero et al., 2005). Dechorionated embryos were fixed in 2% gluteraldehyde and 0.5% paraformaldeheyde in 0.1 M phosphate buffer overnight at 4°C.

Two-photon excitation timelapse microscopy

Two-photon imaging was performed as described (Ulrich et al., 2003). Details can be provided on request.

Movement analysis in two dimensions

To analyze YSN and microsphere movements in two dimensions (2D), we used previously described Motion Tracking software (Helenius et al., 2006; Rink et al., 2005). Net dorsal speed was calculated by dividing the net displacement in the *x*-axis by the total time. We used the emerging notochord and neural tube as anatomical landmarks to determine the embryonic midline.

Movement analysis in three dimensions

To analyze nuclear and cell movements in three dimensions (3D), we implemented an automated tracking algorithm, allowing the estimation of nuclear trajectories without user interaction (Stühmer, 2007).

Similarity quantification

In this section we refer to a cell, nucleus or bead generically as an 'element' for convenience, as the same algorithm is used to quantify movement of all three. The velocity of element i at time point t_k can be estimated from the displacement between two consecutive timepoints as

$$\vec{v}_i(t_k) = \frac{\vec{x}_i(t_k) - \vec{x}_i(t_{k-1})}{t_k - t_{k-1}} ,$$

where $\vec{x}_i(t)$ is the position of the center of element i at time t. To quantify the correlation between the movement of two elements, we calculated the instant similarity measure (Costa Lda et al., 2005). The similarity between the motion of element i and a neighboring element j at time t can be defined as the normalized internal product of the corresponding velocity vectors, yielding the cosine of the smallest angle between these vectors:

$$S_{ij}(t) = \frac{\langle \vec{v}_i(t), \vec{v}_j(t) \rangle}{|\vec{v}_i(t)||\vec{v}_j(t)|} = \cos\theta .$$

Elements moving with parallel velocity give the maximum similarity of 1.0, whereas elements moving in different directions give smaller values. A value of –1.0 indicates movement in opposite directions.

Because the image segmentation algorithm that is used for automated tracking in 3D depends on the image resolution, estimated positions can adopt only discrete values. The resulting quantization error is especially large in the *z*-direction. To reduce this effect of quantization noise, the positions are filtered along the trajectory with a mean filter kernel that averages over the four previous and future time points.

Distance difference quantification

To analyze the movement of iYSN in the presence of mesendoderm progenitors in our transplantation experiments, we calculated the normalized distance difference $\Delta d_{ij}(t)$ between each nearest-neighbor iYSN/mesendoderm progenitor pair (i,j) at consecutive time points.

$$\Delta d_{ij}(t) = \frac{d_{ij}(t_k) - d_{ij}(t_{k-1})}{d_{ij}(t_k) + d_{ij}(t_{k-1})} ,$$

where $d_{ij}(t) = |\vec{x}_j(t) - \vec{x}_i(t)|$. A value of zero indicates that the distance stays constant over the time interval. Positive or negative values indicate that the iYSN and progenitor are moving towards or away from each other, respectively.

Flow field analysis

The flow fields were computed with the FlowJ plugin for ImageJ (NIH, USA) (Abramoff et al., 2000), using the Lucas-Kanade method (Lucas and Kanade, 1981). Flow vectors where drawn using a custom-built vector field visualization plugin for ImageJ that exports the computed vectors into SVG (Scalable Vector Graphics) format.

Hydrodynamic description of progenitor-induced cortical flow

By investigating the constitutive properties of the cortex and the length and time scales involved in progenitor migration, we develop a suitable physical description of YSN dynamics. The cytoskeleton is viscoelastic, displaying elastic behavior on short time scales and viscous behavior on long time

scales. The time scale for elastic relaxation is system dependent, though typical values are of the order of seconds to minutes (Pullarkat et al., 2007), e.g. ≈40 seconds for chick fibroblasts (Thoumine and Ott, 1997). The time scale for cortical flow induced by a transplanted patch of progenitors is given by $a/U_p \approx 50$ minutes, where $a \approx 50$ μm is the radius of a progenitor patch and $U_p \approx 1$ μm/minute is the speed with which the progenitor patch moves. Since the time scale for cortical flow is much longer than that for elastic relaxation, the cortex may be described as an incompressible viscous fluid for the present purpose. In general, the flow profile is a function of the Reynolds number (the ratio of inertial to viscous forces) and the system geometry (Landau and Lifshitz, 1987). We overestimate the Reynolds number as $Re=\rho U_p a/\eta \approx 10^{-5}$, where ρ is the density, which we take to be that of water, and η is the viscosity, which we underestimate to be 10× that of water, approximately the measured viscosity of cytoplasm in tissue culture cells (Luby-Phelps, 2000) (the viscosity of the cortex is expected to be much higher). To specify the geometry, we model the cortex as an infinite 2D fluid in the plane immediately below the progenitor patch. We specify that the fluid in contact with the patch moves with a velocity U, whereas the rest of fluid is free to move, satisfying the boundary conditions that the velocity is U at the edge of the patch and zero infinitely far away. This is equivalent to flow past a circle, for which approximate solutions for the flow profile are known for low Re (Lamb, 1932; Van Dyke, 1975). Importantly, in the low Re regime, the velocity decays from the progenitor patch very slowly as log r, r being the distance from the patch. Finally, we verify that the YSN move along with the cortical flow (advectively), as opposed to diffusively, by estimating the Péclet number, $Pe=Ua/D$, the ratio of diffusive to advective time scales, where D is the diffusivity. To estimate D, we use the Stokes-Einstein-Sutherland relation with an effective viscosity of ≈1 Pa-s, interpreted from measurements of microspheres in fibroblasts (Luby-Phelps, 2000), giving $D \approx 10^{-4}$ μm^2/s. This is an underestimation of D, as the YSN are larger than the 0.16 μm beads described previously (Luby-Phelps, 2000), resulting in greater effective viscosity. Nevertheless, we obtain $Pe \approx 50$, which means that advection dominates diffusion and the YSN move with the progenitor-induced cortical flow.

RESULTS

iYSN and mesendoderm progenitors undergo coordinated convergence movements

Previous studies in zebrafish have suggested that iYSN undergo convergence movements similar to mesendoderm progenitors overlying the YSL during gastrulation (D'Amico and Cooper, 2001). To quantitatively determine the extent to which iYSN and mesendoderm convergence movements are coordinated, we recorded timelapse movies of paraxial and lateral regions of gastrulating zebrafish embryos in which we fluorescently labeled iYSN and nuclei of overlying mesendoderm progenitors (Fig. 1A-C). To analyze and compare the trajectories of iYSN and mesendoderm cells, we developed an image analysis software that allows automated tracking of nuclei in three dimensions (3D) over time (Fig. 1C-F; Movie 1) (Stühmer, 2007). We quantified movement coordination between iYSN and mesendoderm progenitors by determining the similarity between the movements of mesendoderm cells and iYSN at short (0-40 μm), medium (40-80 μm) and long (80-120 μm) distances. The similarity value corresponds to the cosine of the smallest angle between two velocity

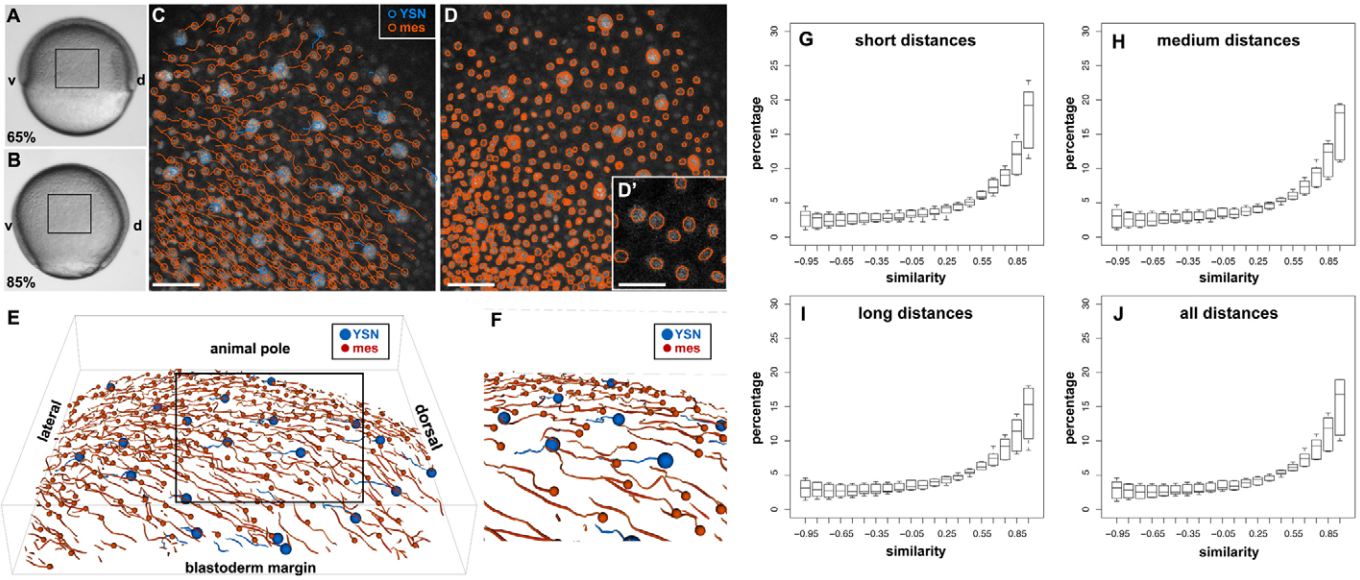

Fig. 1. Convergence movements are highly coordinated between iYSN and mesendoderm. (**A**,**B**) Bright-field images of an embryo at the beginning of gastrulation (6.5 hpf; A) and at mid-gastrulation (8.5 hpf; B). Animal pole is towards the top and dorsal is towards the right. Boxes delineate the imaged region in C-E. (C,E,F) Trajectories of iYSN and mesendoderm progenitors during gastrulation were obtained by imaging embryos by 2-photon excitation microscopy from 65% epiboly stage (6.5 hpf) until 85% epiboly stage (8.5 hpf), and analyzing these movies with a newly developed 3D tracking software. Dorsal is towards the right and circles indicate the endpoint of each track. (**C**) *Z*-projection showing iYSN (blue tracks) and mesendoderm (orange tracks) nuclear trajectories. (**D**) *Z*-projection depicting the efficacy of the image segmentation algorithm to detect nuclei in 3D. (**D'**) Magnification of a single slice of the image in D. The segment boundaries (in orange) are plane cuts of the ellipsoids detected by the image segmentation algorithm. Large ellipsoids represent iYSN, small ellipsoids represent cell nuclei. (**E**,**F**) 3D views of the trajectories of iYSN (blue tracks) and mesendoderm progenitors (orange tracks). (F) Magnification of boxed region in E. (G-J) Quantification of similarity values between iYSN and mesendoderm progenitors in wild-type embryos at mid-gastrulation stages (7-8 hpf). Histograms of the similarity values were generated separately for each embryo (n=6 embryos). Box plots show the distribution of the bin heights among the different embryos. (**G**) Similarity at short distances (0-40 μm). On average, 52% of the values are higher than 0.5. (**H**) Similarity at medium distances (40-80 μm). On average, 50% of the values are higher than 0.5. (**I**) Similarity at long distances (80-120 μm). On average, 48% of the values are higher than 0.5. (**J**) Similarity distribution considering all distances together. On average, 50% of the values are higher than 0.5. d, dorsal; v, ventral; mes, mesendoderm. Scale bars: 50 μm in C,D; 25 μm in D'.

vectors (Costa Lda et al., 2005). Thus, cells and iYSN moving in the same direction will have high similarity values (close to 1), whereas cells and iYSN moving in opposite directions will have low similarity values (close to –1). We found that for short distances 52% of values were higher than 0.5, indicating high movement similarity (Fig. 1G). The similarity values were only slightly reduced for medium and long distances (Fig. 1H,I), suggesting that movement coordination of iYSN and mesendoderm slowly decays with increasing distance. We also determined movement similarity among iYSN and among mesendoderm progenitors, and found a high degree of movement similarity in both cases (see Fig. S1 in the supplementary material). These observations indicate that cellular and nuclear movements are highly coordinated not only between the mesendoderm and YSL, but also within each layer. In addition, we observed that mesendoderm progenitors move faster than the underlying iYSN [v(mesendoderm)=1.46 μm/minute; v(iYSN)= 1.06 μm/minute; P<0.05, n=6 embryos]. Taken together, our observations extend previous findings (D'Amico and Cooper, 2001) and show that iYSN and mesendoderm progenitors exhibit highly coordinated convergence movements over long length scales during gastrulation.

iYSN converge by dorsal-directed cortical flow

To obtain insight into the coordination between iYSN and mesendoderm progenitor movements, we investigated how iYSN move within the YSL. It has previously been shown (Solnica-Krezel and Driever, 1994) that the YSL contains a dense network of microtubules where iYSN are embedded. To test whether microtubules might be involved in iYSN movements, we recorded timelapse movies of the microtubule network by expressing a GFP fusion of the microtubule-associated protein Tau in the YSL (Geldmacher-Voss et al., 2003; Kaltschmidt et al., 2000) (see Movie 2 in the supplementary material). The movement of labeled microtubules in relation to iYSN was analyzed by determining the microtubule flow pattern (for details, see Materials and methods) and comparing it with the movement of iYSN therein. We found that during later stages of gastrulation (8-10 hpf), the YSL microtubule network converges towards the dorsal side, similar to the iYSN (Fig. 2A,D), suggesting that iYSN move together with the microtubule network rather than along microtubules. This view was supported by our observation that the movements of the plus ends of microtubules, visualized by expressing a GFP fusion of the microtubule plus end-binding protein 3 (EB3) (Nakagawa et al., 2000; Stepanova et al., 2003) in the YSL, did not exhibit any preferential orientation within the YSL and that iYSN did not show any obvious plus end-directed movements (Fig. 2B,E; see Movie 3 in the supplementary material). To determine whether convergence movements are restricted to iYSN and microtubules, we recorded timelapse movies of cortical actin movements, visualized by expressing Lifeact-GFP (Riedl et al., 2008) (see Movie 4 in the supplementary material). Similar to the iYSN and the microtubule network, cortical actin exhibited

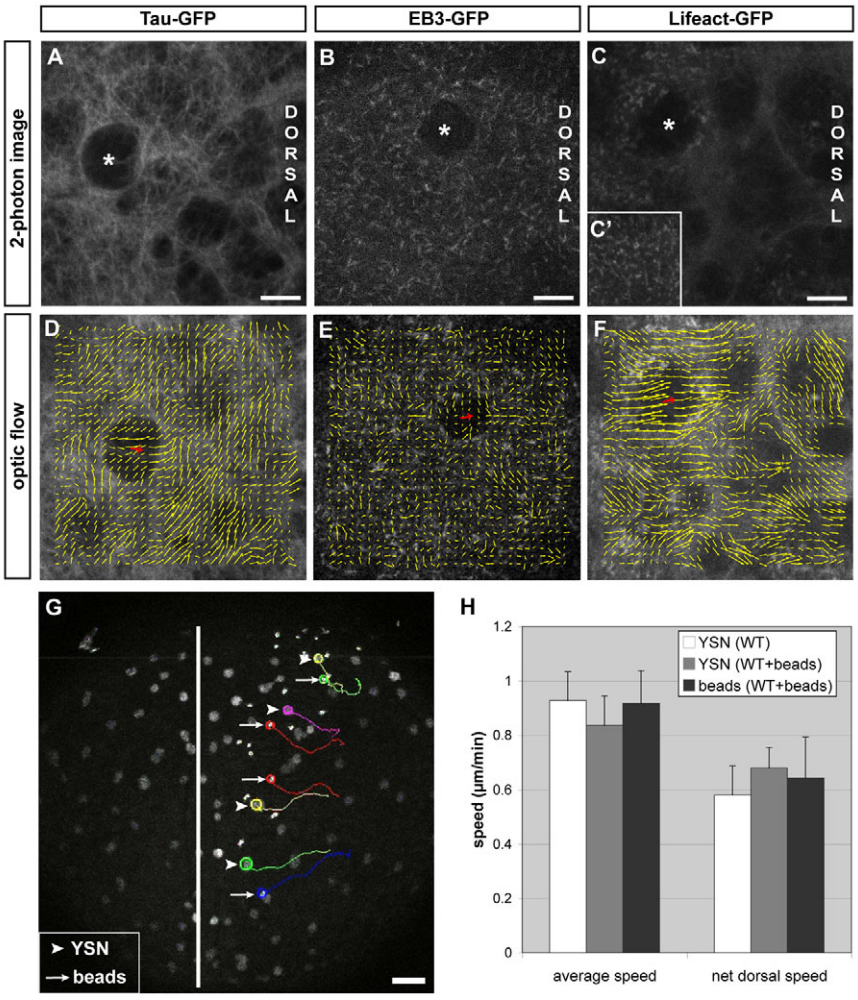

Fig. 2. iYSN converge by cortical flow within the YSL. (**A-C'**) Microtubules labeled with Tau-GFP (A), microtubule plus-ends labeled with EB3-GFP (B) and actin labeled with Lifeact-GFP (C,C') in the paraxial region of the iYSL at 90% epiboly (9 hpf; A,C) and bud stage (10 hpf; B). Asterisks mark iYSN. (C') Dotty actin staining in more superficial layers of the YSL and filamentous actin in deeper layers (C). (**D-F**) Vector fields showing optical flow direction (yellow arrows) of Tau-GFP (D), EB3-GFP (E) and Lifeact-GFP (F). Red arrows indicate the movement direction of the iYSN. (**G**) Two-photon image of two-somite stage wild-type embryo with fluorescently labeled YSN and 0.5 μm diameter fluorescent microspheres injected into the YSL. Image is a z-projection. Several nuclear (arrowheads) and microsphere (bead) trajectories (arrows) obtained using Motion Tracking Software are shown. Circles indicate the endpoint of each track. The white line indicates the dorsal midline of the embryo. (**H**) Comparison of the speed of YSN and bead movements in control embryos (n=6 embryos) and embryos injected with beads (n=2 embryos). No significant differences were found in average and net dorsal speed of YSN and beads (P>0.05). Notably, injected beads appear to have slightly less persistent movements compared with adjacent iYSN (see Movie 4 in the supplementary material). This reduction in bead persistence is probably due to the smaller diameter of the beads (0.5 μm) compared with iYSN (6–20 μm), resulting in greater diffusive relative to advective motion for beads in comparison with iYSN. Dorsal is towards the right (A-F) and animal is towards the top (A-G). Scale bars: 10 μm in A-C; 50 μm in G.

pronounced convergence movements (Fig. 2C,F), indicating that the actin and microtubule cytoskeleton undergo convergence movements together.

These observations suggest that iYSN converge passively together with the YSL cytoskeleton, rather than independently within the YSL. To test whether there is indeed cortical flow within the YSL that could account for iYSN convergence, we injected fluorescently labeled polystyrene microspheres (diameter 0.5 μm) into the YSL and recorded their movements during gastrulation. To analyze these timelapses, we automatically tracked the movements of iYSN and injected microspheres in two dimensions (2D) (Fig. 2G; see Movie 5 in the supplementary material). We observed that the injected beads moved at a similar speed and converged to the dorsal side as their neighboring iYSN (Fig. 2H). This supports the hypothesis that iYSN converge together with the actin and microtubule cytoskeleton by cortical flow towards the dorsal side of the embryo.

Mesendoderm progenitors direct iYSN convergence movement

The observation that iYSN and mesendoderm progenitors exhibit highly coordinated convergence movements during gastrulation suggests interaction between the two. To test whether mesendoderm progenitors are required for iYSN convergence movements, we investigated iYSN movements in *MZoep* mutant embryos, which lack most of their mesendoderm progenitors (Gritsman et al., 1999). By analyzing iYSN movement of *MZoep* embryos in 2D at late gastrulation stages (8-11 hpf), we found that mutant iYSN from lateral and ventral regions of the gastrula exhibited strongly reduced convergence movements compared with wild-type embryos (Fig. 3A,B,D-F; Movies 6-10; see Table S1 in the supplementary material) (D'Amico and Cooper, 2001). To quantify the degree of convergence of iYSN movements, we calculated their net speed along the dorsoventral axis. We found that, in *MZoep*, the net dorsal speed is significantly lower than in wild type (Fig. 3C; see Table S1 in the supplementary material). By contrast, longitudinal YSN movements in dorsal regions appeared largely unchanged in mutant embryos from early to mid-gastrulation stages (6-8 hpf; data not shown). In late gastrulation stages (8-11 hpf), longitudinal movements of mutant iYSN in dorsal regions occurred predominantly in an anterior direction, whereas dorsal iYSN in wild-type embryos undergo longitudinal movements in both anterior and posterior directions (Fig. 3A,B) (D'Amico and Cooper, 2001).

Notably, injection of microspheres into the YSL of mutant embryos revealed that similar to iYSN movements, the convergent cortical flow was strongly reduced in *MZoep* mutants, suggesting that mesendoderm influences iYSN convergence movements by modulating cortical flow (see Fig. S2 and Movie 11 in the supplementary material). To exclude the possibility that Oep protein itself is needed within the YSL for iYSN movements independently of the presence or absence of mesendoderm progenitors, we injected *oep-flag mRNA* (Zhang et al., 1998) into the YSL of *MZoep* mutant embryos. We observed no rescue of the *MZoep* iYSN mutant phenotype in the YSL-injected embryos (see Fig. S3, Table S1 and Movie 12 in the supplementary material).

Endoderm progenitors have previously been suggested to move in close contact to the YSL plasma membrane (Warga and Nusslein-Volhard, 1999). To test whether endoderm progenitors are specifically required for iYSN convergence, we analyzed *casanova* (*cas*) mutant embryos, which lack endoderm but not mesoderm progenitors (Alexander et al., 1999; Dickmeis et al., 2001; Kikuchi et al., 2001). In contrast to the situation in *MZoep* mutant embryos, iYSN convergence movements appear largely unaffected in *cas* mutants (see Fig. S4 and Movie 13 in the supplementary material), indicating that endoderm progenitors are not specifically required for iYSN convergence. Taken together, these data suggest a crucial function of mesoderm progenitors in iYSN convergence movements.

Although these findings demonstrate a requirement for mesendoderm progenitors in iYSN convergence, they do not indicate whether mesendoderm progenitors are also sufficient to direct iYSN convergence movements. To address a possible instructive function of mesendoderm for iYSN movement, we transplanted a small number of blastodermal cells into the lateral side of *MZoep* mutant embryos and monitored the movements of

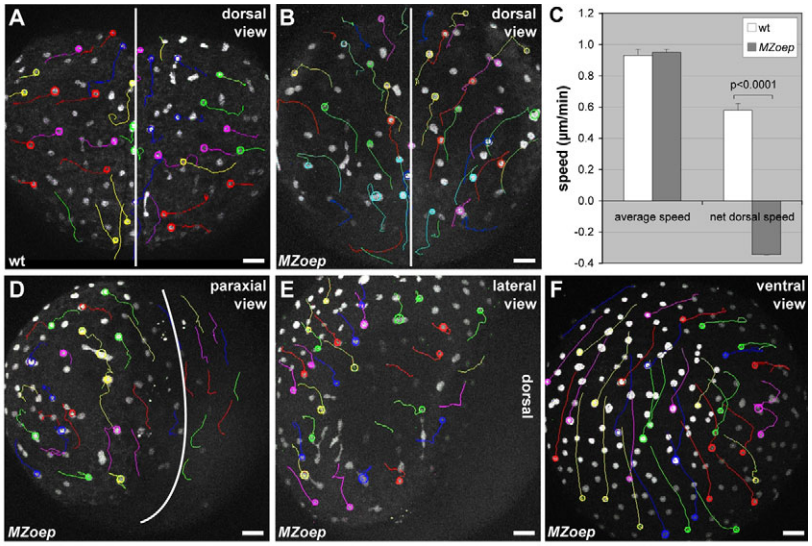

Fig. 3. iYSN convergence movements are impaired in *MZoep* mutant embryos. (A,B,D-F) iYSN trajectories in wild-type (A) and *MZoep* (B,D-F) embryos at the two-somite stage (11 hpf) in dorsal (A,B), paraxial (D), lateral (E) and ventral (F) view. Images are *z*-projections. Some of the nuclear trajectories obtained using Motion Tracking Software are shown. Circles indicate the endpoint of each track. The white lines in A,B,D mark the dorsal midline of the embryo. Animal pole is towards the top. (**A**) In wild-type (wt) embryos, iYSN converge from lateral and paraxial regions towards the dorsal side of the embryo, and undergo longitudinal movements along the anteroposterior axis of the gastrula. (**B**) In *MZoep*, iYSN from lateral and paraxial regions fail to converge to the dorsal side, but still undergo longitudinal movements in an anterior direction. (**C**) Comparison of the speed of iYSN movements between wild-type (wt) and *MZoep* embryos. The average speed of iYSN is similar in wild-type and *MZoep* embryos [P=0.7412; n=6 (wt); n=2 (*MZoep*)]. By contrast, the net dorsal speed is significantly lower in *MZoep* embryos compared with wild type [P<0.0001; n=6 (wt); n=2 (*MZoep*)]. The negative *MZoep* value indicates that the net dorsal movement of the nuclei is away from the dorsal midline. Unpaired Student's *t*-tests were performed to test the differences between mean values. Error bars represent the standard error of the mean. (**D-F**) iYSN from paraxial, lateral and ventral regions in *MZoep* mutants show little convergence movements to the dorsal side. In F, the embryo is slightly tilted, and thus some lateral iYSN are observed on the right side of the image moving away from the dorsal region.

iYSN relative to the position of the transplanted cells. The majority of these cells underwent ingression and expressed mesendodermal markers, as previously reported (Carmany-Rampey and Schier, 2001) (data not shown), indicating that they adopt a mesendodermal fate. From mid-gastrulation stages onwards, the transplanted cells converged toward the dorsal side (Fig. 4; see Movies 14 and 16 in the supplementary material). Strikingly, iYSN in the transplanted side of *MZoep* mutant embryos converged together with the transplanted cells, whereas iYSN on the opposite, non-transplanted side continued to show only very reduced convergence movements (Fig. 4A-E; see Movies 15 and 16 in the supplementary material). This was confirmed when we determined the net dorsal speed of iYSN movement in the presence and absence of transplanted cells (Fig. 4C; see Table S1 in the supplementary material). To analyze the convergence movements of iYSN relative to the transplanted cells in more detail, we imaged the transplanted region at higher magnifications and tracked their movements in 3D (Fig. 4F,G; see Movie 14 in the supplementary material). We found that, as in wild-type embryos, iYSN and transplanted cells move with high similarity values (see Materials and methods) at short as well as at long distances (Fig. 4H,I). These results suggest that convergence movements of mesendoderm progenitors are able to induce convergence movements of underlying iYSN.

E-cadherin is required for coordination of iYSN and mesendoderm convergence movements

Questions remain as to the molecular and cellular mechanisms by which mesendoderm progenitors interact with the YSL to direct iYSN convergence. To determine whether physical contact between YSL and mesendoderm progenitors is required, we visualized the contact zone between mesendoderm progenitors and iYSL using transmission electron microscopy. We found that the plasma membranes of the iYSL and overlying mesendoderm progenitors were often directly adjacent to each other and showed electron-dense structures resembling adherens junctions (Fig. 5A).

E-cadherin (*cdh1* gene in zebrafish) has previously been shown to be highly expressed in the YSL and mesendoderm progenitors, and to represent a key component regulating cell-cell interaction both within and between the forming germ layers during gastrulation (Fig. 5B) (Babb and Marrs, 2004; Kane et al., 2005; Krieg et al., 2008; McFarland et al., 2005; Montero et al., 2005; Shimizu et al., 2005). To determine whether E-cadherin is also required for the coordination of iYSN and mesendoderm progenitor convergence movements, we interfered with E-cadherin expression by injecting a previously characterized morpholino oligonucleotide (MO) targeted against *e-cadherin* and monitored iYSN and mesendoderm convergence movements in 3D over time. We analyzed the movements of iYSN and mesendoderm at mid-gastrulation stages

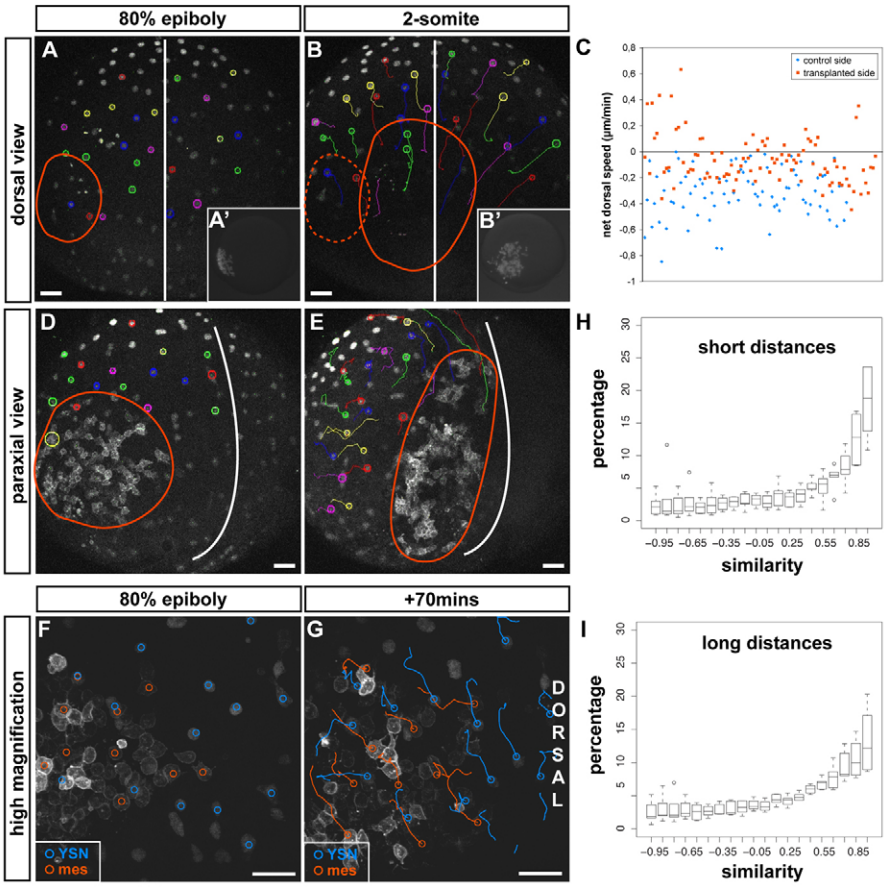

Fig. 4. Mesendoderm directs iYSN convergence movements. (A,B,D,E) Trajectories of iYSN in *MZoep* embryos containing transplanted mesendoderm cells at 80% epiboly (8 hpf; A,D, startpoint of tracks) and at the two-somite stage (11 hpf; B,E, endpoint of tracks). The red line marks the position of the transplanted cells. (**A**,**B**) iYSN convergence movements at the side of *MZoep* embryos containing transplanted mesendoderm cells versus iYSN on the untransplanted side. Dorsal view. (**A'**,**B'**) Images of rhodamine dextran-labeled transplanted cells in the same *MZoep* embryo in A,B before (8 hpf; A') and after (11 hpf; B') the timelapse. (**C**) Quantification of iYSN net dorsal speed shows that iYSN convergence movements at the side containing transplanted mesendoderm cells is significantly increased compared with the convergence of iYSN at the untransplanted side ($P<0.0001$; $n=197$ iYSN from four embryos). Unpaired Student's *t*-tests were performed to test the differences between the mean values. (**D**,**E**) Paraxial view of a transplanted *MZoep* embryo shows that lateral iYSN moving behind the transplanted cells (labeled with membrane-bound GFP) undergo convergence movements similar to the transplanted cells. (**F**,**G**) Trajectories of iYSN (blue tracks) and transplanted cells labeled with membrane-bound GFP (orange tracks) in a transplanted *MZoep* embryo at 80% epiboly (8 hpf; F, startpoint of tracks) and 70 minutes later (G, endpoint of tracks). Images are *z*-projections. Dorsal is towards the right and animal is towards the top. iYSN underneath and in front of the transplanted cells move dorsally and posteriorly together with the cells. (**H**,**I**) Quantification of movement similarity between iYSN and transplanted cells. Histograms of the similarity values were generated separately for each experiment ($n=6$). Boxplots show the distribution of the bin heights among the experiments. Circles indicate outliers. (H) Similarity at short distances (0-40 µm). On average, 54% of the values are higher than 0.5. (I) Similarity at long distances (80-120 µm). On average, 48% of the values are higher than 0.5. Considering all distances together, 50% of the values are higher than 0.5 (not shown). Scale bars: 50 µm.

(7-8 hpf) (Fig. 5C; see Movie 17 in the supplementary material) and found that the similarity values for movement coordination between iYSN and mesendoderm were reduced in morphant embryos compared with wild-type embryos. In the morphants, only 35% of the values were higher than 0.5, in contrast to the 50% observed in the wild type (compare Fig. 5E with Fig. 1J). In addition, we observed that mesendoderm progenitors moved slightly slower in *e-cadherin* morphant embryos than in wild-type embryos (see Table S2 in the supplementary material). To verify that the effects in the morphant embryos are specifically due to the loss of E-cadherin function, we also analyzed previously described *e-cadherin* loss-of-function mutants (*weg*) (Kane et al., 1996; Kane et al., 2005) (Fig. 5D; see Movie 18 in the supplementary material). In *weg* mutant embryos, the similarity values for movement coordination between iYSN and mesendoderm were also diminished (35% of the values higher than 0.5) (Fig. 5F), congruous with our observations in *e-cadherin* morphant embryos. Taken together, these data suggest that E-cadherin expression is needed to coordinate iYSN with mesendoderm progenitor cell movements.

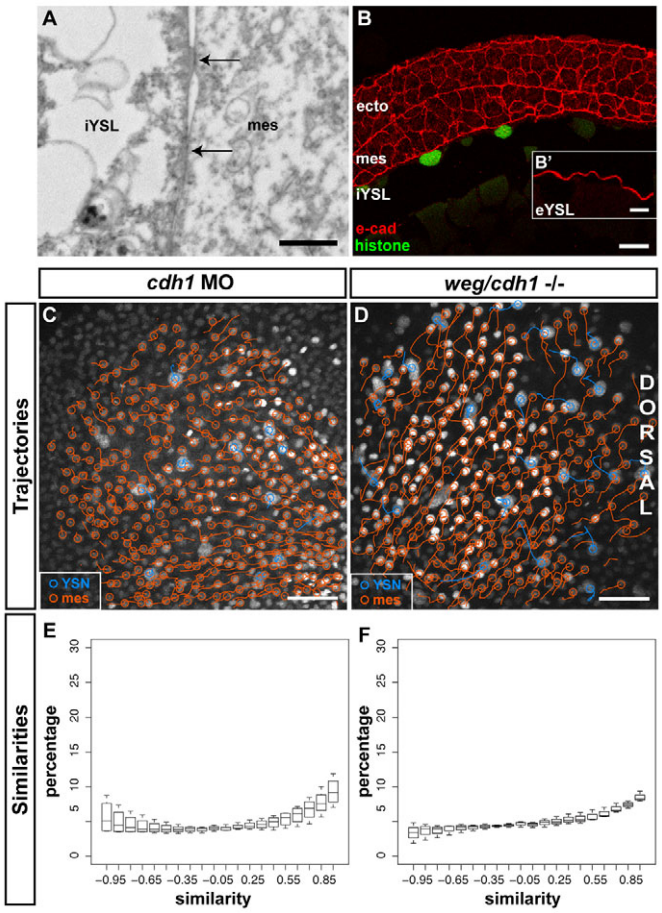

Fig. 5. E-cadherin is required for convergence movement coordination between iYSN and mesendoderm. (**A**) Sagittal section obtained by transmission electron microscopy of a wild-type embryo at 80% epiboly stage (8 hpf) showing a mesendoderm progenitor in close contact with the iYSL plasma membrane. Note the presence of electron-dense regions (arrows) of tight contact between the mesendoderm progenitor and the iYSL plasma membrane. Animal pole is towards the right. (**B**) E-cadherin antibody staining of transversal (B) and sagittal (B′) sections of wild-type gastrulating embryos. E-cadherin is localized at ectoderm, mesendoderm and YSL plasma membranes. (**B′**) Magnification of the eYSL region. (**C**,**D**) Trajectories of iYSN (blue tracks) and mesendoderm progenitors (orange tracks) in *e-cadherin* morphant (C) and *weg*/*e-cadherin* mutant (D) embryos at mid-gastrulation stages (7-8 hpf). Images are *z*-projections. Dorsal is towards the right. (E,F) Quantification of the similarity between iYSN and mesendoderm convergence movements in *e-cadherin* morphants (E) and *weg*/*e-cadherin* mutants (F) at mid-gastrulation stages (7-8 hpf). Histograms of the similarity values were generated separately for each embryo. Boxplots show the distribution of the bin heights among the embryos. (**E**) In *e-cadherin* morphants, 35% of the similarity values are higher than 0.5 (*n*=4 embryos). (**F**) In *weg*/*e-cadherin* mutants, 35% of the similarity values are higher than 0.5 (*n*=3 embryos). e-cad, e-cadherin; ecto, ectoderm progenitor; mes, mesendoderm progenitor. Scale bars: 2 μm in A; 20 μm in B; 10 μm in B′; 50 μm in C,D.

E-cadherin is dynamically linked to the actin cortex of cells (Adams and Nelson, 1998; Gumbiner, 2005). This, together with our previous observation that iYSN move together with the actin and microtubule cytoskeleton by cortical flow, suggests that E-cadherin coordinates mesendoderm progenitor and iYSN movements by interacting with the YSL actin cytoskeleton. To determine whether partial disruption of the actin cytoskeleton can phenocopy loss of E-cadherin function in this process, we incubated embryos with the actin depolymerizing drug cytochalasin B during gastrulation, which has previously been shown to effectively interfere with the actin cytoskeleton in the zebrafish gastrula (Zalik et al., 1999) (see Movies 19 and 4 in the supplementary material). When we analyzed iYSN and mesendoderm movements in cytochalasin B-treated embryos (Fig. 6A,C; see Movie 20 in the supplementary material), we found reduced similarity values for movement coordination between iYSN and mesendoderm when compared with wild-type embryos (only 34% of the values were higher than 0.5) (Fig. 6E), similar to the situation in *e-cadherin* mutants and morphants. To test whether polymerized actin is required locally within the YSL, we injected the actin-polymerizing drug phalloidin (Cooper, 1987; Wehland et al., 1977) directly into the YSL. We found that phalloidin effectively interfered with actin distribution within the YSL (compare Fig. 6B with Fig. 2C; see Movies 21 and 4 in the supplementary material) and that the similarity values for movement coordination between mesendoderm and iYSN were reduced in phalloidin-injected embryos compared with wild-type embryos (only 41% of the values were higher than 0.5) (Fig. 6D,F; see Movie 22 in the supplementary material). This suggests that polymerized actin within the YSL plays a crucial function in this process. Taken together, these results suggest that mesendoderm control of iYSN convergence movements requires E-cadherin expression and that the YSL actin cytoskeleton plays an important function therein.

Mesendoderm progenitors induce convergent cortical flow within the YSL

The observation that mesendoderm progenitors are required and sufficient to direct iYSN convergence movements suggests a function of mesendoderm progenitors in iYSN movements. It has previously been hypothesized that YSN movements might be driven by chemotactic signals emanated by mesendodermal cells in the hypoblast (Cooper and Virta, 2007). To test this hypothesis, we quantified the distance difference between each iYSN migrating ahead of the transplanted cells (considering the direction of movement of the cells) and its nearest neighboring transplanted mesendoderm progenitor. If the iYSN have the tendency to move toward the transplanted cells, as a result of a chemotactic signal, their distance should decrease over time (for details, see Materials and methods). We found that the normalized distance difference between consecutive timepoints was equally distributed around 0

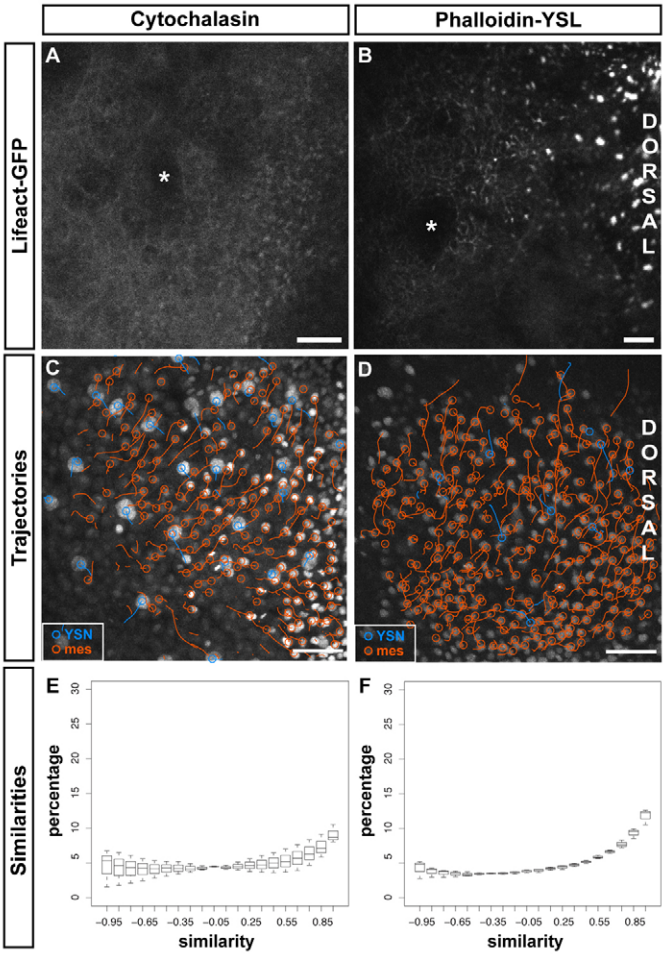

Fig. 6. Filamentous actin within the YSL is required for convergence movement coordination between iYSN and mesendoderm. (**A**,**B**). Actin labeled with Lifeact-GFP in embryos incubated in cytochalasin (A) and injected with Phalloidin into the YSL (B) at 90% epiboly (9 hpf; A) and bud stage (10 hpf; B). Asterisks mark iYSN. (**C**,**D**) Trajectories of iYSN (blue tracks) and mesendoderm progenitors (orange tracks) in cytochalasin-treated (C) and phalloidin YSL-injected (D) embryos at mid-gastrulation stages (7-8 hpf). Images are *z*-projections. Dorsal is towards the right. (**E**,**F**) Quantification of the similarity between iYSN and mesendoderm convergence movements in cytochalasin-treated (E) and phalloidin YSL-injected (F) embryos at mid-gastrulation stages (7-8 hpf). Histograms of the similarity values were generated separately for each embryo. Box plots show the distribution of the bin heights among the embryos. (E) In cytochalasin-treated embryos, 34% of the similarity values are higher than 0.5 (*n*=3 embryos). (F) In phalloidin YSL-injected embryos, 41% of the similarity values are higher than 0.5 (*n*=3 embryos). mes, mesendoderm progenitor. Scale bars: 2 μm in A; 20 μm in B; 50 μm in C,D.

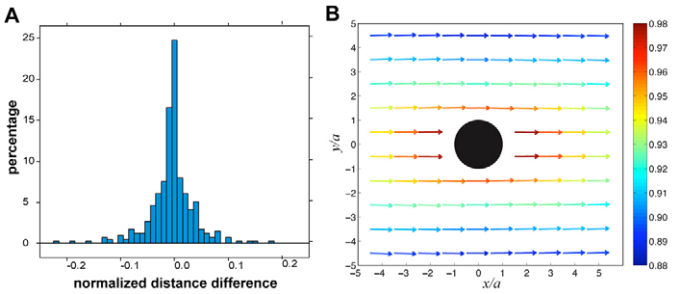

Fig. 7. Movements of iYSN in relation to the transplanted mesendoderm cells can be explained by a cortical flow mechanism. (**A**) Normalized distance difference between iYSN and their nearest mesendoderm progenitor neighbor at consecutive timepoints. The equal distribution of the values around the mean of –0.003±0.027 indicates that, on average, iYSN and transplanted cells keep a constant distance between each other while moving. (**B**) Depiction of cortical flow near a circular patch of transplanted mesendoderm progenitors of radius *a* moving at velocity *U* (black circle) from Lamb's solution for low *Re* flow past a cylinder (Lamb, 1932; Van Dyke, 1975; Veysey and Goldenfeld, 2007). The length and color of the arrows indicate the cortical velocity in units of *U*. The effect of the cells is felt far away, with the velocity only having decayed about 10% over a distance equal to three patch radii.

(exact mean value=–0.003±0.027) (Fig. 7A), indicating that iYSN and transplanted cells keep a constant distance between each other. These results argue against mesendoderm progenitors directly attracting iYSN, e.g. through the release of a chemotactic signal.

Instead of attracting iYSN by chemotactic signaling, converging mesendoderm progenitors might direct iYSN convergence by creating a dorsal-directed cortical flow within the underlying YSL cytogel. Our finding that E-cadherin-mediated adhesion between mesendoderm and YSL is involved in this process suggests that converging mesendoderm progenitors create this cortical flow by dragging the YSL plasma membrane and associated cortical cytoskeleton. To investigate the plausibility of this hypothesis, we considered the force balances for this system. First, we noted that for mesendoderm progenitors to exert a force on the YSL, they must have a substrate for migration other than the YSL itself. Consistent with this, we have previously shown that anterior axial mesendoderm progenitors can use the overlying non-internalizing ectoderm progenitors as a substrate on which to migrate (Montero et al., 2005). Next, we analyzed the propagation of forces exerted by a transplanted patch of cells on the YSL cortex. Modeling the cortex as a 2D viscous fluid and the patch of cells as a translating solid material, we found (1) that the forces exerted by the patch are long range, inducing cortical flow even far away from the progenitors (see Fig. 7B for the flow profile), and (2) that the YSN are advected with this induced flow (for details, see Materials and methods). Indeed, the convergence movement of the YSN in our transplantation experiments displays this behavior, supporting the hypothesis that transplanted mesendoderm progenitors induce iYSN convergence movements by modulating cortical flow within the YSL.

DISCUSSION

In zebrafish, iYSN and overlying mesendoderm progenitors have been suggested to undergo similar convergence movements during gastrulation (D'Amico and Cooper, 2001). Here, we show that mesendoderm progenitors control iYSN convergence movements by modulating cortical flow within the YSL responsible for iYSN transport. Furthermore, we provide evidence that the coordination between mesendoderm and iYSN convergence movements depends on E-cadherin expression, suggesting that adhesive contact between mesendoderm and YSL is involved.

Previous studies have demonstrated that YSN undergo both epiboly and convergence and extension movements (D'Amico and Cooper, 2001; Solnica-Krezel and Driever, 1994; Trinkaus, 1951). Furthermore, interfering with the actin and microtubule cytoskeleton of the YSL has been shown to disrupt epiboly movements of the

YSL (Cheng et al., 2004; Hsu et al., 2006; Koppen et al., 2006; Solnica-Krezel and Driever, 1994; Zalik et al., 1999), suggesting a crucial function of the cytoskeleton for YSN epiboly. By contrast, the role of the YSL cytoskeleton for iYSN convergence and extension movements had not yet been addressed. Our observation that iYSN, together with the actin and microtubule cytoskeleton converge by cortical flow within the YSL indicates that iYSN are not actively transported along microtubules, as has been demonstrated for other types of nuclear migrations (Morris, 2000; Morris, 2003; Reinsch and Gonczy, 1998; Xiang and Fischer, 2004). Instead, the actin and microtubule cytoskeleton appear to function simply as a medium in which the iYSN are entrained and advected. This notion is further supported by our observation that beads injected into the YSL undergo convergence movements similar to neighboring iYSN. These findings are reminiscent of previous experiments in the rainbow trout, demonstrating that chalk particles implanted into the YSL cytoplasm undergo pronounced convergence movements (Long, 1980).

Observations in *Drosophila* suggest that cytoplasmic streaming is involved in nuclear distribution within the syncytial preblastoderm and in mixing and dispersal of cytoplasmic components within the oocyte (Dahlgaard et al., 2007; Serbus et al., 2005; Theurkauf, 1994; von Dassow and Schubiger, 1994). The mechanisms underlying cortical flow within the YSL are currently unknown. However, it is conceivable that, analogous to the situation in the *Drosophila* preblastoderm (von Dassow and Schubiger, 1994), acto-myosin contraction combined with local changes in actin polymerization within the YSL controls this streaming. Whether iYSN converge solely by cortical flow or whether other transport mechanisms also contribute to iYSN convergence is presently unclear. Our preliminary observations of iYSN being stretched and pulled apart (not shown) suggest that there are cytoskeletal forces that pull on the nuclear envelope and possibly contribute to iYSN movements.

During gastrulation, highly organized cell and tissue movements lead to the formation of the embryonic body axis (Solnica-Krezel, 2005; Stern, 1992). Consistent with this and previous observations (D'Amico and Cooper, 2001), we found that in gastrulating zebrafish embryos cellular and nuclear movements of mesendoderm and YSL are highly coordinated. Furthermore, our observations suggest that iYSN convergence movements depend on mesendoderm convergence and that mesendoderm directs iYSN convergence movements. Interestingly, YSN have previously been shown to undergo epiboly movements independently of the overlying blastoderm in zebrafish and killifish (*Fundulus*) (Kane et al., 1996; Trinkaus, 1951; Trinkaus, 1984). This apparent difference in blastoderm dependence between epiboly and convergence movements of YSN is probably due to different processes controlling these movements. Although YSN epiboly has been proposed to depend on parallel filaments of microtubules polarized towards the vegetal pole (Solnica-Krezel and Driever, 1994), we show that iYSN convergence movements are directed by cortical flow through contact with the overlying mesendoderm. Our observation that microspheres injected into the YSL strongly converge to the dorsal side, while showing only very reduced epiboly movements (not shown) points at the interesting possibility that YSN epiboly involves active nuclear migration, whereas iYSN convergence does not.

Previous studies have hypothesized that iYSN movements might be driven by chemotactic signals emanating from mesendodermal cells in the hypoblast (Cooper and Virta, 2007). However, we found no evidence for mesendoderm attracting neighboring iYSN, arguing against the assumption that mesendoderm directs iYSN convergence through chemotactic signaling. By contrast, we provide evidence that iYSN converge by cortical flow within the YSL and that mesendoderm progenitors control this cortical flow through E-cadherin-mediated contact with the YSL. Mesendoderm progenitors most probably establish a physical link to the YSL plasma membrane via E-cadherin, which then enables mesendoderm progenitors undergoing convergence movements to drag the YSL plasma membrane and associated cortical cytoskeleton in the same direction. In such a scenario, E-cadherin-mediated adhesion between mesendoderm and YSL would be required to establish sufficient friction between these layers to allow the effective pulling of the mesendoderm on the YSL. The plausibility of this notion is supported by our hydrodynamic analysis showing that the flow of a viscous fluid induced by a solid patch moving over its surface closely resembles the cortical flow within the YSL induced by mesendoderm progenitors moving over it.

Questions remain about the specific role of coordinated convergence movements of the blastoderm and underlying iYSN during embryogenesis. Clearly, transcription from iYSN is crucial for a variety of different embryonic processes, ranging from mesendoderm cell fate induction to heart progenitor cell migration (Chen and Kimelman, 2000; Mizuno et al., 1999; Mizuno et al., 1996; Ober and Schulte-Merker, 1999; Rodaway et al., 1999; Sakaguchi et al., 2006). In addition, dorsally restricted expression of the homeobox transcription factor *hex* within the iYSL has been associated with dorsoventral patterning of the gastrula, suggesting that the spatially regulated transcription of this gene within the YSL is important for its activity (Ho et al., 1999).

Future experiments will have to determine whether iYSN convergence movements are indeed required for blastoderm patterning and/or morphogenesis by specifically interfering with iYSN convergence movements within the YSL.

We are grateful to M. Wilsch-Bräuninger for advice and assistance with electron microscopy, and to B. Flach for supervising the development of the image segmentation algorithm. We also thank J. Peychl for advice and assistance with confocal and two-photon excitation microscopy, S. Grill for advice and assistance with the fluid flow analysis, T. Pietzsch for advice with the Kalman Filter, and G. Junghanns, E. Lehmann and J. Hückmann for fish care. We thank M. Köppen, A. Oates, S. Saalfeld, G. Soete and P. Tomancak for critical reading of the manuscript. This work was supported by grants from the Human Frontier Science Program to J.S.B., and the Deutsche Forschungsgemeinschaft, European Community (ZF-Models, Endotrack, ZF-Cancer), and Max-Planck-Society to C.P.H.

Supplementary material

Supplementary material for this article is available at
http://dev.biologists.org/cgi/content/full/136/8/1305/DC1

References

Abramoff, M. D., Niessen, W. J. and Viergever, M. A. (2000). Objective quantification of the motion of soft tissues in the orbit. *IEEE Trans. Med. Imaging* **19**, 986-995.

Adams, C. L. and Nelson, W. J. (1998). Cytomechanics of cadherin-mediated cell-cell adhesion. *Curr. Opin. Cell Biol.* **10**, 572-577.

Alexander, J., Rothenberg, M., Henry, G. L. and Stainier, D. Y. (1999). casanova plays an early and essential role in endoderm formation in zebrafish. *Dev. Biol.* **215**, 343-357.

Babb, S. G. and Marrs, J. A. (2004). E-cadherin regulates cell movements and tissue formation in early zebrafish embryos. *Dev. Dyn.* **230**, 263-277.

Baker, J., Theurkauf, W. E. and Schubiger, G. (1993). Dynamic changes in microtubule configuration correlate with nuclear migration in the preblastoderm Drosophila embryo. *J. Cell Biol.* **122**, 113-121.

Carmany-Rampey, A. and Schier, A. F. (2001). Single-cell internalization during zebrafish gastrulation. *Curr. Biol.* **11**, 1261-1265.

Chen, S. and Kimelman, D. (2000). The role of the yolk syncytial layer in germ layer patterning in zebrafish. *Development* **127**, 4681-4689.

Cheng, J. C., Miller, A. L. and Webb, S. E. (2004). Organization and function of microfilaments during late epiboly in zebrafish embryos. *Dev. Dyn.* **231**, 313-323.

Cooper, J. A. (1987). Effects of cytochalasin and phalloidin on actin. *J. Cell Biol.* **105**, 1473-1478.
Cooper, M. S. and Virta, V. C. (2007). Evolution of gastrulation in the ray-finned (actinopterygian) fishes. *J. Exp. Zool. B Mol. Dev. Evol.* **308**, 591-608.
Costa Lda, F., Cintra, L. C. and Schubert, D. (2005). An integrated approach to the characterization of cell movement. *Cytometry A* **68**, 92-100.
D'Amico, L. A. and Cooper, M. S. (2001). Morphogenetic domains in the yolk syncytial layer of axiating zebrafish embryos. *Dev. Dyn.* **222**, 611-624.
Dahlgaard, K., Raposo, A. A., Niccoli, T. and St Johnston, D. (2007). Capu and Spire assemble a cytoplasmic actin mesh that maintains microtubule organization in the Drosophila oocyte. *Dev. Cell* **13**, 539-553.
Dickmeis, T., Mourrain, P., Saint-Etienne, L., Fischer, N., Aanstad, P., Clark, M., Strahle, U. and Rosa, F. (2001). A crucial component of the endoderm formation pathway, CASANOVA, is encoded by a novel sox-related gene. *Genes Dev.* **15**, 1487-1492.
Englander, L. L. and Rubin, L. L. (1987). Acetylcholine receptor clustering and nuclear movement in muscle fibers in culture. *J. Cell Biol.* **104**, 87-95.
Foe, V. E. and Alberts, B. M. (1983). Studies of nuclear and cytoplasmic behaviour during the five mitotic cycles that precede gastrulation in Drosophila embryogenesis. *J. Cell Sci.* **61**, 31-70.
Geldmacher-Voss, B., Reugels, A. M., Pauls, S. and Campos-Ortega, J. A. (2003). A 90-degree rotation of the mitotic spindle changes the orientation of mitoses of zebrafish neuroepithelial cells. *Development* **130**, 3767-3780.
Gonzalez-Reyes, A., Elliott, H. and St Johnston, D. (1995). Polarization of both major body axes in Drosophila by gurken-torpedo signalling. *Nature* **375**, 654-658.
Gritsman, K., Zhang, J., Cheng, S., Heckscher, E., Talbot, W. S. and Schier, A. F. (1999). The EGF-CFC protein one-eyed pinhead is essential for nodal signaling. *Cell* **97**, 121-132.
Gumbiner, B. M. (2005). Regulation of cadherin-mediated adhesion in morphogenesis. *Nat. Rev. Mol. Cell Biol.* **6**, 622-634.
Helenius, J., Brouhard, G., Kalaidzidis, Y., Diez, S. and Howard, J. (2006). The depolymerizing kinesin MCAK uses lattice diffusion to rapidly target microtubule ends. *Nature* **441**, 115-119.
Ho, C. Y., Houart, C., Wilson, S. W. and Stainier, D. Y. (1999). A role for the extraembryonic yolk syncytial layer in patterning the zebrafish embryo suggested by properties of the hex gene. *Curr. Biol.* **9**, 1131-1134.
Hsu, H. J., Liang, M. R., Chen, C. T. and Chung, B. C. (2006). Pregnenolone stabilizes microtubules and promotes zebrafish embryonic cell movement. *Nature* **439**, 480-483.
Kaltschmidt, J. A., Davidson, C. M., Brown, N. H. and Brand, A. H. (2000). Rotation and asymmetry of the mitotic spindle direct asymmetric cell division in the developing central nervous system. *Nat. Cell Biol.* **2**, 7-12.
Kane, D. A., Hammerschmidt, M., Mullins, M. C., Maischein, H. M., Brand, M., van Eeden, F. J., Furutani-Seiki, M., Granato, M., Haffter, P., Heisenberg, C. P. et al. (1996). The zebrafish epiboly mutants. *Development* **123**, 47-55.
Kane, D. A., McFarland, K. N. and Warga, R. M. (2005). Mutations in half baked/E-cadherin block cell behaviors that are necessary for teleost epiboly. *Development* **132**, 1105-1116.
Kikuchi, Y., Agathon, A., Alexander, J., Thisse, C., Waldron, S., Yelon, D., Thisse, B. and Stainier, D. Y. (2001). casanova encodes a novel Sox-related protein necessary and sufficient for early endoderm formation in zebrafish. *Genes Dev.* **15**, 1493-1505.
Kimmel, C. B. and Law, R. D. (1985). Cell lineage of zebrafish blastomeres. II. Formation of the yolk syncytial layer. *Dev. Biol.* **108**, 86-93.
Koppen, M., Fernandez, B. G., Carvalho, L., Jacinto, A. and Heisenberg, C. P. (2006). Coordinated cell-shape changes control epithelial movement in zebrafish and Drosophila. *Development* **133**, 2671-2681.
Krieg, M., Arboleda-Estudillo, Y., Puech, P. H., Kafer, J., Graner, F., Muller, D. J. and Heisenberg, C. P. (2008). Tensile forces govern germ-layer organization in zebrafish. *Nat. Cell Biol.* **10**, 429-436.
Lamb, H. (1932). *Hydrodynamics*. Cambridge: Cambridge University Press.
Landau, L. D. and Lifshitz, E. M. (1987). *Fluid mechanics*. London: Pergamon.
Long, W. L. (1980). Analysis of yolk syncytium behavior in *Salmo and Catostomus*. *J. Exp. Zool.* **214**, 323-331.
Luby-Phelps, K. (2000). Cytoarchitecture and physical properties of cytoplasm: volume, viscosity, diffusion, intracellular surface area. *Int. Rev. Cytol.* **192**, 189-221.
Lucas, B. D. and Kanade, T. (1981). An iterative image registration technique with an application to stereo vision. In *International Joint Conference on Artificial Intelligence*. p. 674-679. Canada: International Joint Conference on Artificial Intelligence.
McFarland, K. N., Warga, R. M. and Kane, D. A. (2005). Genetic locus half baked is necessary for morphogenesis of the ectoderm. *Dev. Dyn.* **233**, 390-406.
Mizuno, T., Yamaha, E., Wakahara, M., Kuroiwa, A. and Takeda, H. (1996). Mesoderm induction in zebrafish. *Nature* **383**, 131-132.
Mizuno, T., Yamaha, E., Kuroiwa, A. and Takeda, H. (1999). Removal of vegetal yolk causes dorsal deficencies and impairs dorsal-inducing ability of the yolk cell in zebrafish. *Mech. Dev.* **81**, 51-63.
Montero, J. A., Carvalho, L., Wilsch-Brauninger, M., Kilian, B., Mustafa, C. and Heisenberg, C. P. (2005). Shield formation at the onset of zebrafish gastrulation. *Development* **132**, 1187-1198.
Morris, N. R. (2000). Nuclear migration: from fungi to the mammalian brain. *J. Cell Biol.* **148**, 1097-1101.
Morris, N. R. (2003). Nuclear positioning: the means is at the ends. *Curr. Opin. Cell Biol.* **15**, 54-59.
Nakagawa, H., Koyama, K., Murata, Y., Morito, M., Akiyama, T. and Nakamura, Y. (2000). EB3, a novel member of the EB1 family preferentially expressed in the central nervous system, binds to a CNS-specific APC homologue. *Oncogene* **19**, 210-216.
Ober, E. A. and Schulte-Merker, S. (1999). Signals from the yolk cell induce mesoderm, neuroectoderm, the trunk organizer, and the notochord in zebrafish. *Dev. Biol.* **215**, 167-181.
Pullarkat, P. A., Fernandez, P. A. and Ott, A. (2007). Rheological properties of the eukaryotic cell cytoskeleton. *Phys. Rep.* **449**, 29-53.
Reinsch, S. and Gonczy, P. (1998). Mechanisms of nuclear positioning. *J. Cell Sci.* **111**, 2283-2295.
Riedl, J., Crevenna, A. H., Kessenbrock, K., Yu, J. H., Neukirchen, D., Bista, M., Bradke, F., Jenne, D., Holak, T. A., Werb, Z. et al. (2008). Lifeact: a versatile marker to visualize F-actin. *Nat. Methods* **5**, 605-607.
Rink, J., Ghigo, E., Kalaidzidis, Y. and Zerial, M. (2005). Rab conversion as a mechanism of progression from early to late endosomes. *Cell* **122**, 735-749.
Robinson, J. T., Wojcik, E. J., Sanders, M. A., McGrail, M. and Hays, T. S. (1999). Cytoplasmic dynein is required for the nuclear attachment and migration of centrosomes during mitosis in Drosophila. *J. Cell Biol.* **146**, 597-608.
Rodaway, A., Takeda, H., Koshida, S., Broadbent, J., Price, B., Smith, J. C., Patient, R. and Holder, N. (1999). Induction of the mesendoderm in the zebrafish germ ring by yolk cell-derived TGF-beta family signals and discrimination of mesoderm and endoderm by FGF. *Development* **126**, 3067-3078.
Roth, S., Neuman-Silberberg, F. S., Barcelo, G. and Schupbach, T. (1995). cornichon and the EGF receptor signaling process are necessary for both anterior-posterior and dorsal-ventral pattern formation in Drosophila. *Cell* **81**, 967-978.
Sakaguchi, T., Kikuchi, Y., Kuroiwa, A., Takeda, H. and Stainier, D. Y. (2006). The yolk syncytial layer regulates myocardial migration by influencing extracellular matrix assembly in zebrafish. *Development* **133**, 4063-4072.
Serbus, L. R., Cha, B. J., Theurkauf, W. E. and Saxton, W. M. (2005). Dynein and the actin cytoskeleton control kinesin-driven cytoplasmic streaming in Drosophila oocytes. *Development* **132**, 3743-3752.
Shimizu, T., Yabe, T., Muraoka, O., Yonemura, S., Aramaki, S., Hatta, K., Bae, Y. K., Nojima, H. and Hibi, M. (2005). E-cadherin is required for gastrulation cell movements in zebrafish. *Mech. Dev.* **122**, 747-763.
Solnica-Krezel, L. (2005). Conserved patterns of cell movements during vertebrate gastrulation. *Curr. Biol.* **15**, R213-R228.
Solnica-Krezel, L. and Driever, W. (1994). Microtubule arrays of the zebrafish yolk cell: organization and function during epiboly. *Development* **120**, 2443-2455.
Starr, D. A. and Han, M. (2003). ANChors away: an actin based mechanism of nuclear positioning. *J. Cell Sci.* **116**, 211-216.
Stepanova, T., Slemmer, J., Hoogenraad, C. C., Lansbergen, G., Dortland, B., De Zeeuw, C. I., Grosveld, F., van Cappellen, G., Akhmanova, A. and Galjart, N. (2003). Visualization of microtubule growth in cultured neurons via the use of EB3-GFP (end-binding protein 3-green fluorescent protein). *J. Neurosci.* **23**, 2655-2664.
Stern, C. D. (1992). Vertebrate gastrulation. *Curr. Opin. Genet. Dev.* **2**, 556-561.
Stühmer, J. (2007). *Segmentierung von Zellkernen gastrulierender Zebrafischembryonen in 3-dimensionalen Aufnahmen der konfokalen Lasermikroskopie*. Dresden: Faculty of Computer Science, Technische Universität Dresden.
Theurkauf, W. E. (1994). Premature microtubule-dependent cytoplasmic streaming in cappuccino and spire mutant oocytes. *Science* **265**, 2093-2096.
Thoumine, O. and Ott, A. (1997). Time scale dependent viscoelastic and contractile regimes in fibroblasts probed by microplate manipulation. *J. Cell Sci.* **110**, 2109-2116.
Trinkaus, J. P. (1951). A study of mechanism of epiboly in the egg of *Fundulus heteroclitus*. *J. Exp. Zool.* **118**, 269-320.
Trinkaus, J. P. (1984). Mechanism of *Fundulus* epiboly-a current view. *Am. Zool.* **24**, 673-688.
Trinkaus, J. P. (1993). The yolk syncytial layer of Fundulus: its origin and history and its significance for early embryogenesis. *J. Exp. Zool.* **265**, 258-284.
Ulrich, F., Concha, M. L., Heid, P. J., Voss, E., Witzel, S., Roehl, H., Tada, M., Wilson, S. W., Adams, R. J., Soll, D. R. et al. (2003). Slb/Wnt11 controls hypoblast cell migration and morphogenesis at the onset of zebrafish gastrulation. *Development* **130**, 5375-5384.
Van Dyke, M. (1975). *Perturbation Methods in Fluid Mechanics*. Stanford, CA: Parabolic Press.

Veysey, J. and Goldenfeld, N. (2007). Simple viscous flows: from boundary layers to the renormalization group. *Rev. Mod. Phys.* **79**, 883-927.
von Dassow, G. and Schubiger, G. (1994). How an actin network might cause fountain streaming and nuclear migration in the syncytial Drosophila embryo. *J. Cell Biol.* **127**, 1637-1653.
Warga, R. M. and Nusslein-Volhard, C. (1999). Origin and development of the zebrafish endoderm. *Development* **126**, 827-838.
Wehland, J., Osborn, M. and Weber, K. (1977). Phalloidin-induced actin polymerization in the cytoplasm of cultured cells interferes with cell locomotion and growth. *Proc. Natl. Acad. Sci. USA* **74**, 5613-5617.
Westerfield, M. (2000). *The Zebrafish Book: A Guide for the Laboratory Use of Zebrafish (Danio rerio)*. Eugene, OR: University of Oregon Press.
Xiang, X. and Fischer, R. (2004). Nuclear migration and positioning in filamentous fungi. *Fungal Genet. Biol.* **41**, 411-419.
Zalik, S. E., Lewandowski, E., Kam, Z. and Geiger, B. (1999). Cell adhesion and the actin cytoskeleton of the enveloping layer in the zebrafish embryo during epiboly. *Biochem. Cell Biol.* **77**, 527-542.
Zhang, J., Talbot, W. S. and Schier, A. F. (1998). Positional cloning identifies zebrafish one-eyed pinhead as a permissive EGF-related ligand required during gastrulation. *Cell* **92**, 241-251.